Pivot method for global optimization: a study of water clusters $(H_2O)_N$ with $2 \leqslant N \leqslant 33$

Pablo Nigra, Sabre Kais [*]

Department of Chemistry, Purdue University, West Lafayette, IN 47907, USA

Received 10 February 1999; in final form 1 April 1999

Abstract

By means of the pivot method, an optimization work on water clusters $(H_2O)_N$, with $2 \leqslant N \leqslant 33$, is carried out using an ab initio rigid molecule model, the Matsuoka–Clementi–Yoshimine potential, and an empirical flexible molecule model, the Stillinger–Rahman potential. The results show that, under certain conditions, the pivot method algorithm is likely to yield optimized structures that are related to one another in such a manner that they form families. The structures in a family can be thought of as formed from the aggregation of single units to some specific structures. In addition, the sequences present an apparent asymptotic behavior. © 1999 Elsevier Science B.V. All rights reserved.

1. Introduction

Water clusters have been studied since long ago in order to analyze the interactions between water molecules and to develop a deeper understanding of liquid and solid phases of bulk water. Many experimental works concentrate mainly on small water clusters with $N \leqslant 10$ [1–7], whereas theoretical studies cover this range and beyond [8–24]. Among these theoretical studies several potential functions are used to describe the global minimum structures and energies of small clusters as well as to study the properties of liquid water [24–32]. The nature of these potentials ranges from purely ab initio to totally empirical, and the accuracy of their predictions shows different degree of success. One thing in common among these potentials is the complexity of

the surfaces they span. This fact creates the necessity of having efficient methods to explore such surfaces when the global minimum structures are searched.

Recently, Wales and Hodges [22] applied the basin-hopping method to optimize the TIP4P potential [25] for clusters of up to 21 water molecules obtaining the global minimum structures of clusters with $N \leqslant 20$. Then, they used the putative TIP4P global minima to relax the new ASP-W4 potential [32]. A similar analysis is carried out in the present work, but using the pivot method which is an algorithm of easy implementation [33]. In this method, the phase space is initially seeded with a number of random probes, though a priori information about the system can be very useful. Then, the probes are paired according to a nearest neighbor arrangement to immediately choose the probes with the lower energies in each pair as the pivot probes; the others being relocated around the pivots utilizing a generalized q-distribution function [33]. The process is re-

---
[*] Corresponding author. E-mail: kais@power1.chem.purdue.edu

peated by the algorithm until the stopping criteria is reached.

The pivot method has not been previously used for water clusters, and here is applied to two well-known potentials that are very different in nature. One of these potentials is the Matsuoka–Clementi–Yoshimine (MCY) potential [27] that is an ab initio rigid molecule model, the other potential is a central force potential by Stillinger and Rahman (SR) [29] that is an empirical flexible molecule model. The details of these potentials can be found elsewhere [27,29]. It is known that they suffer from some deficiencies, as for example many-body effects, that prevent them from giving accurate results. However, they still can predict structural properties of the condensed phases of water; the MCY potential being more reliable than the SR potential in this respect [34]. The use of the two different potentials is to compare the behavior of structural properties in the finite-size case. Besides, to a first test of the pivot method algorithm in the water cluster optimization problem, they are good representatives of two general models, rigid or flexible water molecules, of somewhat simple functional forms with relatively low computational costs.

In the following, the potentials are optimized for clusters with 2 up to 33 water molecules.

2. Results and discussion

The application of the pivot method to the MCY potential determines a cyclic structure for the trimer, tetramer, and pentamer; a cage-like structure for the hexamer and heptamer; a D_{2d} cubic structure for the octamer; and a cubic structure for the nonamer (with a S_4 underlying octamer). All these in agreement with previous works [15,17,19]. Here D_{2d} and S_4 are point group symmetry forms of the octamer.

For the SR potential, the algorithm determines a cyclic structure for the trimer and the tetramer, and a D_{2d} cubic structure for the octamer in accordance with previous reports [13,23]. The structure for the SR pentamer is found to be a fused ring type that is also found by Plummer et al. [13]. These authors also report a cage-like structure lower in energy than that of the fused rings. All the cage-like structures found by the pivot method are about 1 kcal mol^{-1} higher

in energy than that of the fused rings. The structure of the SR hexamer is a distorted triangular prism (structure II of Ref. [8]) even lower in energy than that given by Güvenç and Anderson [23]. The SR heptamer has the same cage-like structure to that of the MCY heptamer while the SR nonamer is cubic (with a D_{2d} underlying octamer).

The results for larger clusters show that the found minimum structures of the clusters present a certain regular behavior for both potentials. That is, the clusters are built from some specific structures and have the cyclic tetramers as building units. Further-
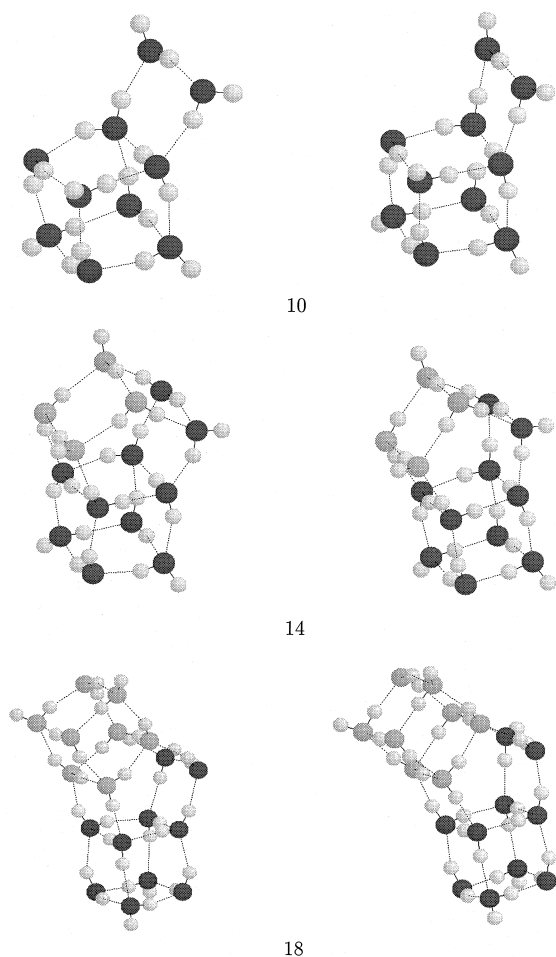

Fig. 1. Some clusters of group 3. MCY left, SR right. Going from top to bottom, it can be seen that each cluster differs in size by a cyclic tetramer from the cluster immediately below. Note that the decamers embedded in the 18-mers are structural isomers of the decamers at the top of the figure.
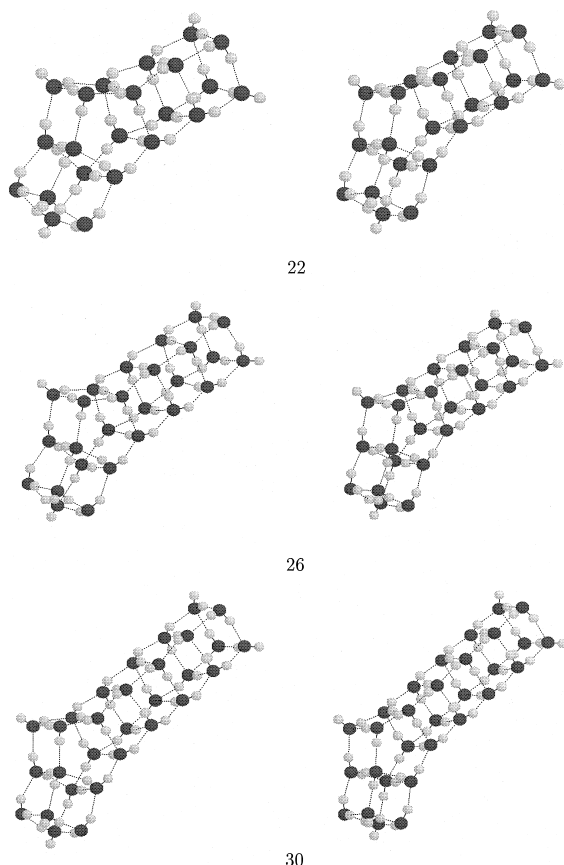
22

26

30

Fig. 2. Clusters of group 3. MCY left, SR right. The aggregation of cyclic tetramer tends to form a D_{2d} fused-cube branch.

more, the clusters are arranged in such a way that they form four different groups characterized by a parameter k_i. The groups can be expressed as:

$$N_i = 4n + k_i, \qquad (1)$$

where N_i is the number of molecules of a cluster in the group i; n, which takes on positive integers, is the number of tetramers that comprise the cluster; and k_i, which assumes integer values from 0 to 3, is a parameter. Indeed, these values for k_i represent the number of extra molecules to be added to the building tetramers.

It is clear from Eq. (1) that the specific structures from which the clusters of each group are built are: the tetramer for group 1, the pentamer for group 2, the hexamer for group 3, and the heptamer for group 4. The dimer and trimer can be included in groups 3

and 4, respectively, if n is allowed to take also on 0 in these two groups.

Fig. 1 shows some representative clusters of group 3 ($k_3 = 2$). Going from top to bottom in the figure, it is noted that each cluster differs in size by a cyclic tetrameric unit from the cluster immediately below. This behavior is observed again in clusters of groups 1 and 2, but not in clusters of group 4. Another feature common to groups 1, 2, and 3 is that the process of joining cyclic tetramers to a structure to build larger clusters favors the formation of a D_{2d} fused-cube branch. Fig. 2 shows this feature clearly for clusters of group 3. To be more specific, if the cyclic tetramers are attached to the left branch of the 22-mers in Fig. 2, the energies of the resultant 26-mers and 30-mers are higher than those of the respective 26-mers and 30-mers shown in the same figure. The structures of group 4 are not simply related to each other, which is an indication of the complexity of the potential surfaces for these clusters using both MCY and SR potentials. However, most of these structures present a backbone of D_{2d} fused cubes where the extra molecules adhere.

Table 1 shows the energies of some selected configurations compared to the energies of the respective D_{2d} fused-cube structures found by the

Table 1
Energies in kcal mol^{-1} of some selected configurations (see Fig. 3)

Cluster	MCY	SR
10-mer		
$\quad D_{2d}$ fused cubes	−84.714	−84.929
$\quad$ Pentagonal prism	−85.693	−87.165
12-mer		
$\quad D_{2d}$ fused cubes	−107.294	−110.164
$\quad$ Hexagonal prisms	−104.781	−106.570
15-mer		
$\quad D_{2d}$ fused cubes	−134.912	−137.513
$\quad$ Face-sharing pentagonal prisms	−135.929	−142.585
20-mer		
$\quad D_{2d}$ fused cubes	−188.468	−196.488
$\quad$ Face-sharing pentagonal prisms	−187.080	−198.364
$\quad$ Edge-sharing pentagonal prisms	−189.183	−191.157
$\quad$ Dodecahedron	−182.214	−183.586
30-mer		
$\quad D_{2d}$ fused cubes	−290.538	−302.468
$\quad$ Face-sharing pentagonal prisms	−289.493	−309.993
$\quad$ Face-sharing hexagonal prisms	−287.023	−308.710

pivot method. Some of these structures are shown in Fig. 3. It can be concluded that the pivot method does not necessarily reach the global minimum structures. An explanation for this can be given considering the prior information used by the algorithm to optimize a new structure [33]. To optimize a structure with $N \geqslant 10$, the algorithm uses as input the structure of smaller clusters: octamer, nonamer, and so on. These smaller clusters are of cubical form. This situation, together with the fact that the opti-

Fig. 4. Energy per molecule ε in kcal mol^{-1} of the fused-cube structures versus the number of tetramers n comprising the clusters. Note how the curves, including that of group 4 ($k_4 = 3$), seem to converge on the same limit.

mized clusters tend to form a fused-cube branch, suggests that the pivot method is likely to optimize a family of structures if the input consists solely of structures belonging to the same family. In the present case, the structural family consists of linear chains of cyclic tetramers, or fused cubes, whose optimized structures comprise D_{2d} octamers and constitute four different groups described by the set of Eq. (1).

Fig. 4 shows two plots, one for each potential, of the energy per molecule $\varepsilon = |E/N|$ versus the number of tetramers n comprising the clusters which is defined in Eq. (1). The data corresponding to clusters with $N > 33$ are obtained by adding cyclic tetramers to the fused-cube branches of the biggest representative structures of each group, with the exception of that of group 4. Also, the data corresponding to the MCY nonamer in group 2 are those of a D_{2d} type
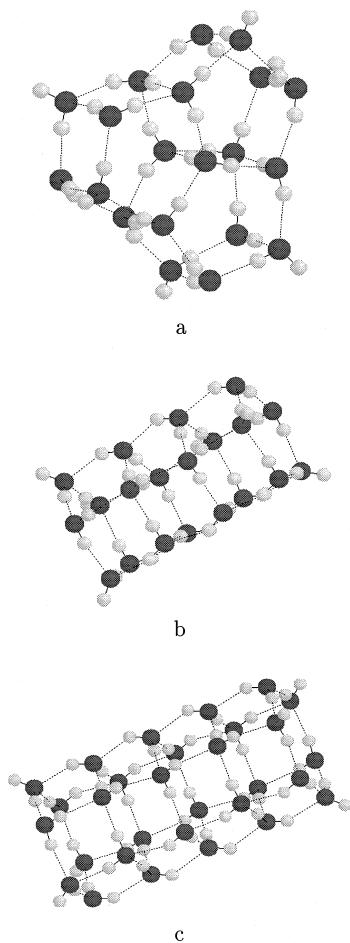

Fig. 3. Some selected structures whose energies are given in Table 1. (a) 20-mer edge-sharing pentagonal prisms. (b) 20-mer face-sharing pentagonal prisms. (c) 30-mer face-sharing hexagonal prisms. As shown in Table 1, these structures may have stabilization energies lower than those of the respective fused-cube structures.
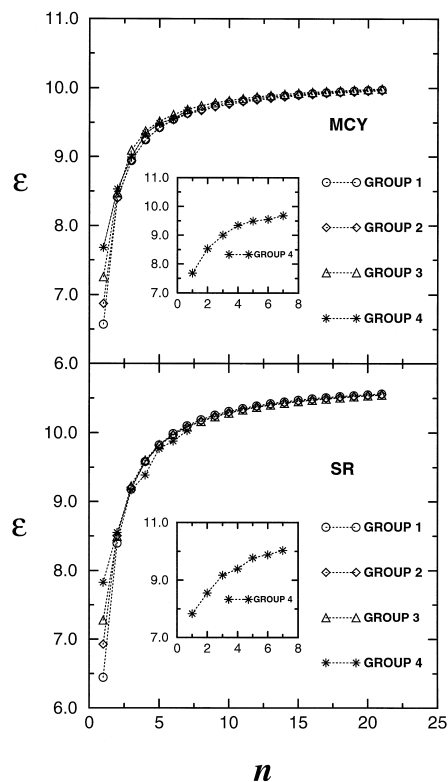
structure like the data of the other structures in the same group. Clearly in Fig. 4, the points corresponding to groups 1, 2, and 3 span smooth curves, respectively, and each of these curves seems to tend towards the same limit when n goes to infinity. For the points representing group 4 which are shown in more detail, the situation is a little different. They do not span a smooth curve, but their dispersion from a smooth one appears to be fairly small. This picture arises when the possible structures, of the same family, of every particular cluster in a given group have similar energies per molecule ε that span very closed curves once in plots like those of Fig. 4. It appears, however, that the points of group 4 follow the same tendency as that noted for the points of groups 1, 2, and 3 when n increases.
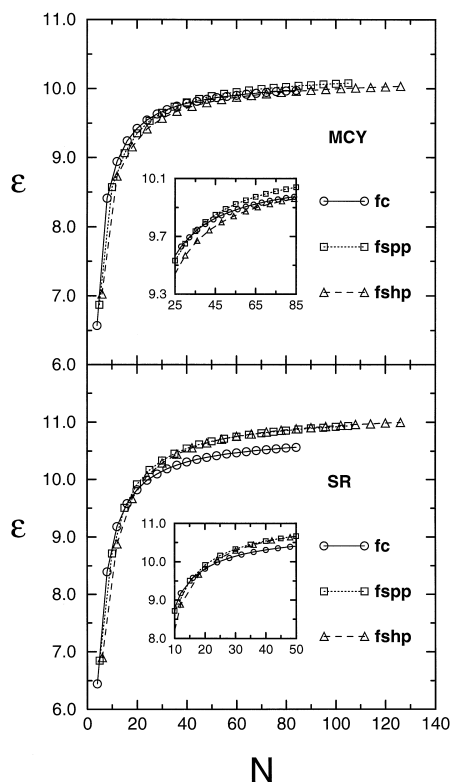
The fact that the lowest energy structures found for the MCY octamer and nonamer are of type D_{2d} and S_4, respectively, along with the data shown in Table 1, suggests that the phenomenon of crossing is possible. After all, the stable cubical structure of the octamer and the most stable phase of ice at $T = 0$ and $P = 0$, hexagonal ice I_h, do not appear to belong to the same family of structures. Fig. 5 shows some crossings among curves of different families where N is the number of water molecules in the cluster. It is clear that the crossings are potential dependent, but it is also clear that the face-sharing pentagonal prism curve and the face-sharing hexagonal prism curve tend to a higher limit of ε than that which the fused-cube curve does. This last feature is more remarkable for the SR curves. Also in the SR case, there is a noticeable crossing between the face-sharing prism curve and the face-sharing hexagonal prism curve. This is not observed for the MCY case within the studied range.

3. Conclusions

If optimizing the potential surface of a water cluster is already an intricate task, no less difficult is attempting to find a connection between the properties of the water clusters. Despite this, the obtained results give some clues. The first observation is on Eq. (1), which gives an account of the members of a given family of structures. It seems reasonable to think that any family can be represented by a set of identities of the type of Eq. (1). Moreover, as shown in Figs. 1 and 3, it seems also reasonable to think that the members of any family may form from the aggregation of some particular units. This idea is directly related to the field of *Cluster Assembled Materials* which deals with bulk materials whose building blocks consist of clusters [35]. Although the building units dealt with in the present work are cyclic, there is no need for these to be so in all the existing families. In fact, if the idea of clusters formed from basic units is kept in mind, the results suggest that the cyclic units interact better if they form linear structures. Therefore, to think of a connection between the finite clusters and the known bulk phases of water, non-cyclic clusters arises as a sensible alternative.

Fig. 5. Energy per molecule ε in kcal mol^{-1} versus the number of water molecules N in the clusters. fshp, face-sharing hexagonal prisms; fspp, face-sharing pentagonal prisms; and fc, fused cubes. Although the crossings are potential dependent, the fused-cube sequences appear to converge on a lower limit of ε in both cases.

Other conclusions that can be drawn from the results pertain to the curves of energy shown in Figs. 4 and 5. Once optimized, a family of structures may span several curves, as many as values of the parameter k_i there are in the set of Eq. (1). All these curves present the same asymptotic behavior (see Fig. 4). Therefore, just one of these curves does suffice for relating the given family to a bulk phase. This represents a simplification of the problem even though the number of existing families still may be a daunting point. In addition, the crossings in Fig. 5 are potential dependent and this fact is ultimately related to how the potentials are fitted. The asymptotic behavior of these curves also depends on the fitting of the potentials and apparently presents a quick convergence.

All the above features are subjects for further studies. The existence of the sequences in both potentials suggests that this is not a behavior of a particular function, but rather a general behavior of the water clusters. Also, the apparent asymptotic behavior suggests a clear relation with bulk phases. Sequences formed from non-cyclic units, or a combination of cyclic and non-cyclic units, which present asymptotic behavior, may be related to some of the known bulk phases. At present, the authors of this Letter focus part of their efforts in that direction.

Acknowledgements

References

[1] K. Kim, K. Jordan, T. Zwier, J. Am. Chem. Soc. 116 (1994) 11568.

[2] K. Liu, M. Brown, C. Carter, R. Saykally, J. Gregory, D. Clary, Nature 381 (1996) 501.

[3] K. Liu, J. Cruzan, R. Saykally, Science 271 (1996) 929.

[4] C. Gruenloh, J. Carney, C. Arrington, T. Zwier, S. Fredericks, K. Jordan, Science 276 (1997) 1678.

[5] R. Fredericks, K. Jordan, T. Zwier, J. Phys. Chem. 100 (1996) 7810.

[6] U. Buck, I. Ettischer, M. Melzer, V. Buch, J. Sadlej, Phys. Rev. Lett. 80 (1998) 2578.

[7] C. Gruenloh, J. Carney, F. Hagemeister, C. Arrington, T. Zwier, J. Chem. Phys. 109 (1998) 6601.

[8] J. Pedulla, K. Kim, K. Jordan, Chem. Phys. Lett. 291 (1998) 78.

[9] L. Sremaniak, L. Perera, M. Berkowitz, J. Chem. Phys. 105 (1996) 3715.

[10] J. Pedulla, F. Vila, K. Jordan, J. Chem. Phys. 105 (1996) 11091.

[11] I. Quintana, W. Ortiz, E. López, Chem. Phys. Lett. 287 (1998) 429.

[12] P. Moore Plummer, T. Chen, J. Phys. Chem. 87 (1983) 4190.

[13] P. Moore Plummer, T. Chen, J. Chem. Phys. 86 (1987) 7149.

[14] P. Moore Plummer, J. Mol. Struct. 417 (1997) 35.

[15] J. Pillardy, K. Olszewski, L. Piela, J. Mol. Struct. 270 (1992) 277.

[16] J. Jensen, P. Krishnan, L. Burke, Chem. Phys. Lett. 260 (1996) 499.

[17] K. Kim, M. Dupuis, G. Lie, E. Clementi, Chem. Phys. Lett. 131 (1986) 451.

[18] M. Masella, J. Flament, J. Chem. Phys. 107 (1997) 9105.

[19] R. Wawak, M. Wimmer, H. Scheraga, J. Phys. Chem. 96 (1992) 5138.

[20] D. Estrin, L. Paglieri, G. Corongiu, E. Clementi, J. Phys. Chem. 100 (1996) 8701.

[21] C. Tsai, K. Jordan, J. Phys. Chem. 97 (1993) 5208.

[22] D. Wales, M. Hodges, Chem. Phys. Lett. 286 (1998) 65.

[23] Z. Güvenç, M. Anderson, Z. Phys. D 36 (1996) 171.

[24] G. Merrill, M. Gordon, J. Phys. Chem. A 102 (1998) 2650.

[25] W. Jorgensen, J. Chandrasekhar, J. Madura, R. Impey, M. Klein, J. Chem. Phys. 79 (1983) 926.

[26] P. Cieplak, P. Kollman, T. Lybrand, J. Chem. Phys. 92 (1990) 6755.

[27] O. Matsuoka, E. Clementi, M. Yoshimine, J. Chem. Phys. 64 (1976) 1351.

[28] U. Niesar, G. Corongiu, E. Clementi, G. Kneller, D. Bhattacharya, J. Phys. Chem. 94 (1990) 7949.

[29] F. Stillinger, A. Rahman, J. Chem. Phys. 68 (1978) 666.

[30] J. Halley, J. Rustad, A. Rahman, J. Chem. Phys. 98 (1993) 4110.

[31] C. Millot, A. Stone, Mol. Phys. 77 (1992) 439.

[32] C. Millot, J. Soetens, M. Costa, M. Hodges, A. Stone, J. Phys. Chem. A 102 (1998) 754.

[33] P. Serra, A. Stanton, S. Kais, Phys. Rev. E 55 (1997) 1162.

[34] M. Morse, S. Rice, J. Chem. Phys. 76 (1982) 650.

[35] P. Jena, S. Khanna, B. Rao, Mat. Sci. For. 232 (1996) 1.